https://dx.doi.org/10.1016/j.conbuildmat.2024.135218

Optimized bio-oil emulsification for sustainable asphalt production: A step towards a low-carbon pavement

Ziye Ma [a, b], Hainian Wang [a,*], Yuanle Li [a], Xu Yang [a], Zhen Leng [c]

[a] *School of Highway, Chang'an University, South 2nd Ring Road Middle Section, Xi'an, Shaanxi, 710064, China*

[b] *Department of Civil and Architectural Engineering, KTH-Royal Institute of Technology, Stockholm, Sweden*

[c] *Department of Civil and Environmental Engineering, The Hong Kong Polytechnic University, Kowloon, Hong Kong*

*Corresponding Author: Hainian Wang (wanghn@chd.edu.cn)

Abstract

Bio-oil, derived from biomass, offers a sustainable alternative to petroleum-based asphalt binders in construction. However, its high oxygen content and temperature sensitivity pose challenges. This study explored the possibility of using emulsification technology to produce and apply emulsified bio-asphalt at a relatively low-temperature, aiming for sustainable high-value utilization. Three preparation processes were proposed in this study, including modification followed by emulsification (Process A), emulsification followed by modification (Process B), and separate emulsification followed by mixing (Process C). Based on the thermal characteristics of bio-oil, the optimal emulsification temperature was determined to be 80±1℃. Through an I-optimal experimental design combined with response surface methodology (RSM), the influence of bio-oil and emulsifier on the performance of emulsified bio-asphalt was investigated for each process. It was found that Process C can leverage the low-temperature extensibility and interfacial adhesion benefits of bio-oil to prepare stable emulsified bio-asphalt with superior comprehensive performance. Based on desirability optimization methodology, the study optimized bio-oil and emulsifier content. The recommended composition is 10.37% bio-oil and 3.53% emulsifier for Process C. Through practical observation, emulsified bio-asphalt production offered environmental benefits, reducing emissions of CO_2 and harmful

gases, particularly VOCs and NOx. Additionally, adopting bio-oil aligned with carbon neutrality goals, potentially sequestering 880,000 tons of carbon annually in China's road construction and maintenance activities.

Key words: Sustainability; Bio-oil; Emulsified bio-asphalt; Cleaner production; Multi-objective optimization; Response surface methodology

Graphical abstract

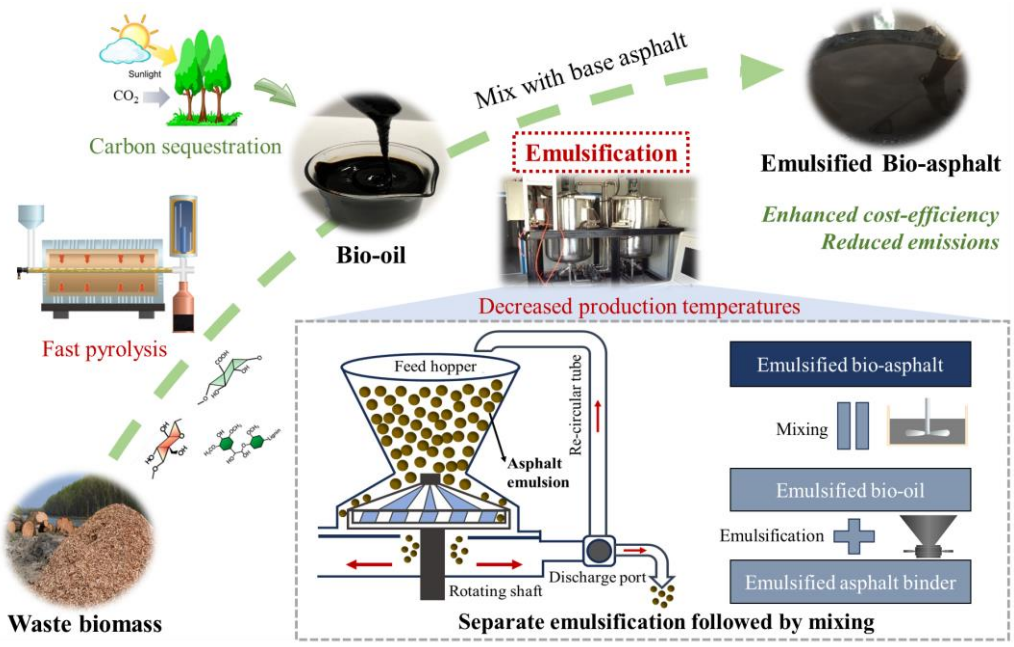

Highlights

- Combining emulsification technology with bio-asphalt can avoid the aging susceptibility of bio-oil.
- Optimal emulsification temperature for bio-oil is 80±1℃ based on its thermal characteristics.
- The process of separate emulsification followed by mixing can leverage the low-temperature extensibility and adhesion benefits of bio-oil.
- The desirability optimization methodology (DOM) is suitable for the multi-objective optimization of emulsified bio-asphalt.
- Emulsified bio-asphalt production offers significant environmental benefits by reducing CO_2 and harmful gas emissions.

1. Introduction

Asphalt binder is a common engineering adhesive used to bond aggregates and is widely employed in various applications such as roads, airports, bridges, and roofing. With the depletion of non-renewable petroleum-based asphalt sources and advancements in refining processes, there is a growing demand for renewable alternative asphalt binders [1, 2]. In recent years, bio-oil derived from fast pyrolysis of biomass materials such as straw, waste wood chips, and animal manure has garnered widespread attention as a potential alternative to petroleum-based asphalt binder, due to its broad availability and environmentally friendly nature [3-5]. Literature evidence demonstrates that the overall production cost of bio-oil, derived from plant biomass, is approximately only $0.54 per gallon [6]. This cost-effectiveness makes large-scale commercial utilization of bio-oil on road construction a viable prospect [7, 8]. Additionally, global carbon-neutral economic incentives and strategies further enhance the attractiveness of bio-based alternatives [9].

However, bio-oil exhibits a typically high oxygen content of up to 30% and an enrichment of light components, which renders it highly sensitive to temperature variations [10, 11]. The hot-mix bio-asphalt binder often exhibits shortcomings in its high-temperature performance and fatigue life, limiting its extensive utilization [12-14]. Moreover, Bio-asphalt binder is susceptible to aging when exposed to oxygen, elevated temperatures, and light, leading to undesirable effects such as brittleness and hardening, as shown in Fig. 1. To overcome the aforementioned limitations of bio-asphalt binder, researchers commonly add polymer modifiers or inorganic fillers to enhance its high-temperature stability, such as polyphosphoric acid (PPA) [15], styrene-butadiene-styrene (SBS) [16, 17], and nano-silica [18]. However, these modifiers often come with high costs, inconsistent properties, and additional processing steps, which may compromise the inherent environmental and economic advantages of bio-oil. In contrast, emulsification technology presents a highly promising solution for efficient utilization of bio-oil. The preparation of emulsified asphalt can be achieved at lower temperatures, preventing the aging of bio-oil and the

volatilization of light components [19]. This approach maximizes the environmental and performance benefits of bio-asphalt binder while capitalizing on the advantages of the emulsification process.

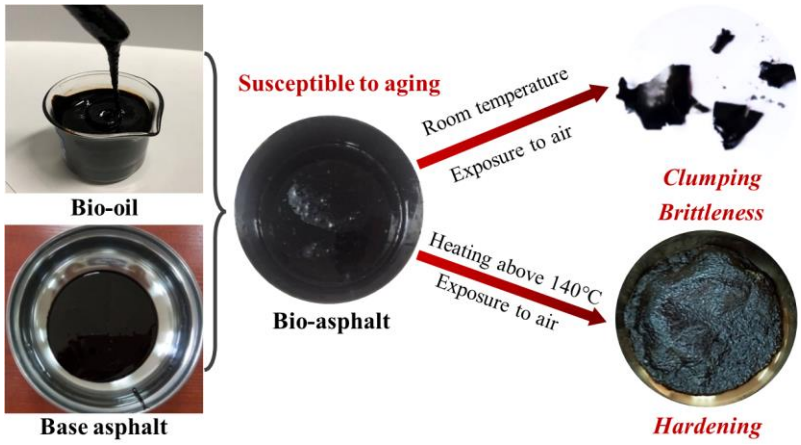

Fig. 1. Limitations of conventional hot-mix bio-asphalt binder

Emulsified asphalt is prepared by subjecting molten asphalt to mechanical shearing, dispersing it into a water-based solution containing emulsifiers and additives, thereby forming an oil-in-water (O/W) system [20, 21]. Asphalt is the main component of asphalt emulsion, typically accounting for 50%-75% of the emulsion. Emulsifiers play a crucial role in preparing asphalt emulsion by reducing the interfacial tension between the oil and water phases and facilitating their emulsification [22]. Cationic emulsifiers are preferred over anionic or non-ionic emulsifiers due to their better adhesion to electronegative siliceous solid aggregates [23]. The quality evaluation of emulsified asphalt mainly focuses on the storage stability and setting behaviors of the emulsion [24, 25], as well as the road performance of the residue [26]. Multiple factors influence the manufacture and performance of emulsified asphalt [27, 28], including the asphalt properties, the type and dosage of emulsifiers, the order of ingredient addition, as well as the temperature and shear rate during manufacturing. The existing research on emulsified asphalt preparation and performance evaluation provides valuable technical support for the development of emulsified bio-asphalt.

Some researchers have preliminarily confirmed the feasibility of emulsified bio-asphalt, with recommended bio-oil content of 15-20% and emulsifier content around 3%

[29]. However, the understanding of emulsified bio-asphalt remains quite limited. For the preparation process, further research is needed to determine the optimal emulsification and modification sequence for bio-oil, as well as the most favorable component ratios. Additionally, a thorough investigation of the interactions among components and their influence on emulsion properties and residue's road performance is essential to achieve a uniform and stable emulsified bio-asphalt system.

In response to these challenges, this study proposed three preparation processes for emulsified bio-asphalt: modification followed by emulsification, emulsification followed by modification, and separate emulsification followed by mixing. The emulsification temperature range was also determined based on the thermal characteristics of the bio-oil. After that, an I-optimal experimental design method was employed innovatively, considering bio-oil content, emulsifier content, and preparation process as control factors. Response surface methodology (RSM) was used to systematically investigate emulsion properties and the road performance of residues. The desirability optimization methodology (DOM) was applied to achieve multi-objective optimization and determine the optimal bio-oil and emulsifier content. Finally, the environmental and economic benefits of emulsified bio-asphalt were assessed. Emission gas detection from the asphalt heating and emulsification processes was conducted, analyzing concentrations of CO_2, SO_2, VOCs, CO, and NOx. On the economic front, a cost analysis was conducted to explore the potential savings and benefits of incorporating bio-oil in road construction and maintenance.

The main objective of this study is to identify the optimal combination of preparation methods and component content in order to achieve a high-performance and easily producible emulsified bio-asphalt. Through practical investigation on emulsification techniques, the study seeks to provide a sustainable solution for the high-value utilization of bio-oil.

2. Experimental procedure

2.1 Raw materials

The bio-oil used in this study was obtained from the fast pyrolysis of waste wood

chips, which was provided by Shandong Tairan Bioengineering Company. As shown in Fig. 2, the bio-oil specimen appeared as a black-brown viscous liquid, with an oxygen element content of 32.8%. During the entire experimental phase, we consistently used the same bio-oil batch to mitigate concerns about variability, ensuring uniform properties were maintained. The basic physical properties of bio-oil were presented in Table 1.

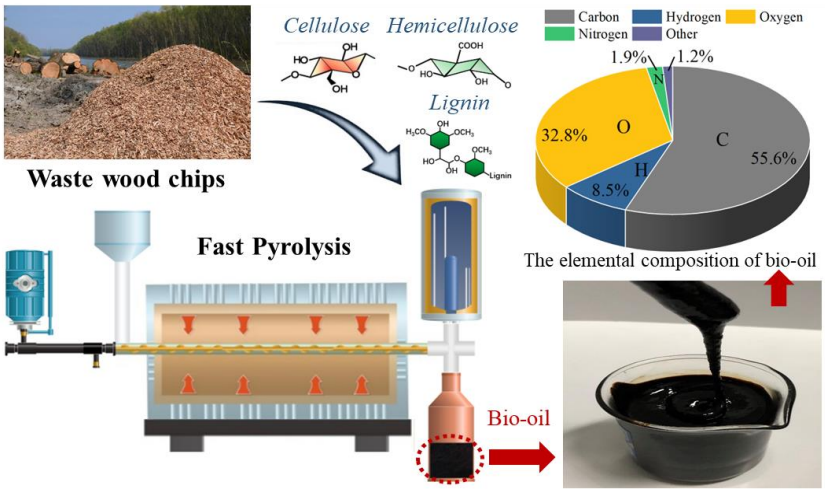

Fig. 2. Acquisition method and elemental composition of wood pyrolysis bio-oil

Table 1 Basic physical properties of bio-oil

Items	Appearance	Density	Viscosity at 60°C	pH	Ash
Test results	Black-brown viscous liquid	1.061 g/cm^3	1.36 Pa·s	3.7	0.1%

The 90# base asphalt binder used to prepare emulsified bio-asphalt was supplied by Shell Company, with conventional properties listed in Table 2. Octadecyl dimethyl ammonium chloride (STAC) was chosen as the cationic emulsifier, supplied by Merck Sigma-Aldrich (China). The STAC emulsifier is a white crystalline powder with a molecular weight of 348.05 and is readily soluble in water. The long carbon chain structure of STAC makes it an ideal ingredient in asphalt emulsifiers. This structural characteristic can enhance the fluidity of the asphalt emulsion, facilitating easier application and reducing the risk of cracks and potholes [30]. Additionally, dilute hydrochloric acid was chosen as the pH regulator to adjust the soap solution's pH to 2. Anhydrous calcium chloride was selected as the stabilizer with a content of 2w% relative to the weight of asphalt.

Table 2 Test results of conventional technical indicators of 90# base asphalt binder

Items		Test value	Requirement
Penetration at 25℃ (0.1 mm)		90.0	80-100
Softening point ($T_{R\&B}$) (℃)		46.8	≥ 45
Ductility at 10℃ (cm)		42.5	≥ 30
Flash point (℃)		265	≥245
Dynamic viscosity at 60℃ (Pa · s)		210	≥160
After RTFO (163℃, 85 min)	Mass variation (%)	-0.47	≤ ±0.8
	Residual penetration ratio at 25℃ (%)	67.4	≥ 57
	Ductility at 10℃ (cm)	12.0	≥ 8

2.2 Emulsification conditions of bio-oil

During the preparation of emulsified bio-asphalt, it is necessary to heat the bio-oil to achieve the desired flowability for emulsification. However, the thermal characteristics of bio-oil tend to be unstable. At room temperature, aldehydes and ketones may undergo reactions, while heating can lead to the volatilization of light components, leading to reduced calorific value and increased viscosity of the bio-oil [31, 32]. Fig. 3 illustrates the thermal characteristics of the bio-oil specimen at different temperatures and storage durations. The results show that the bio-oil maintains relative stability at both 25℃ and 80℃, with a mass loss rate below 6%. When the temperature reaches 90℃, the bio-oil experiences intensified thermal reactions, emitting substantial white smoke accompanied by pungent gases. Due to the evaporation of light components, the bio-oil undergoes severe aging, with a mass loss rate reaching 30% after storage at 100℃ for 3 days. Therefore, the heating temperature during the preparation of emulsified asphalt should not exceed 90℃. In this study, the emulsification temperature was strictly maintained at 80±1℃.

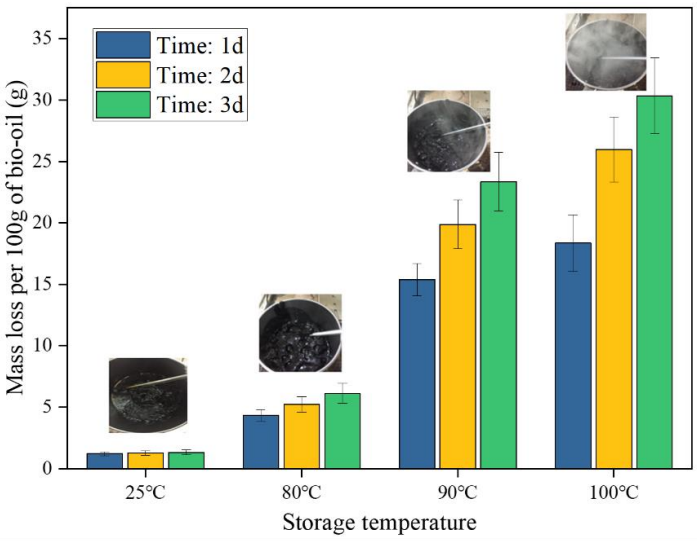

Fig. 3. Thermal storage characteristics of bio-oil

At a preparation temperature of 80°C, the bio-oil flowed smoothly and did not exhibit any undesirable phenomena such as coagulation or agglomeration upon contact with the soap solution. Fig. 4 shows the emulsification effects of bio-oil with varying STAC emulsifier contents (0.5% and 5%). It is evident that the STAC can effectively emulsify the bio-oil, resulting in the formation of well-flowing emulsions. When the emulsifier content reaches 5%, a minor amount of water separation was observed, potentially due to incomplete binding of free emulsifier with the oil phase [33]. Overall, the bio-oil can be effectively subjected to direct emulsification, showing a good compatibility with the soap solution.

Fig. 4. Emulsification effects of bio-oil at different STAC emulsifier contents

2.3 Preparation process

To investigate the influence of the emulsification and modification sequence of bio-oil on emulsified bio-asphalt, three preparation processes were proposed in this study: modification followed by emulsification, emulsification followed by

modification, and separate emulsification followed by mixing. Prior to preparation, the bio-oil was heated at 80°C for 2 hours, while the base asphalt binder was maintained at 140°C for the same duration. The shearing temperature in the colloid mill was set at 80°C, with a shearing fineness of 20μm. Based on previous studies [29], a fixed oil-to-water ratio of 55:45 was maintained in each of the three preparation processes, to ensure the comparability among the experimental outcomes.

(1) Process A: Modification followed by emulsification

As shown in Fig. 5, the procedure initiates by combining preheated bio-oil and base asphalt binder in a high-speed shear mixer. This mixture is subjected to shearing at 4000rpm and 140°C for 10 minutes to produce bio-asphalt binder. Subsequently, the pre-prepared soap solution is introduced into a colloid mill, where the bio-asphalt binder is gradually added in five separate batches. Following previous studies [29], emulsified bio-asphalt can be produced by shearing the mixture at 3500rpm in the colloid mill for 6 minutes.

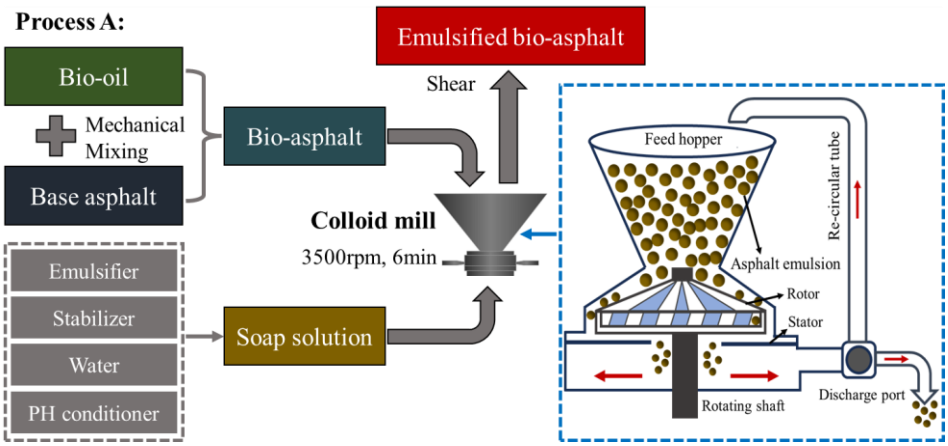

Fig. 5. Preparation process A: Modification followed by emulsification

(2) Process B: Emulsification followed by modification

In Process B, distinct from Process A, we first prepare the emulsified asphalt by blending the base asphalt binder with the soap solution in a colloid mill. This mixture is sheared at 3500 rpm for 6 minutes, ensuring complete emulsification of the base asphalt. Following this, we introduce a specific quantity of bio-oil into the colloid mill containing the emulsified asphalt. The bio-oil is then combined with the emulsified asphalt through additional shearing, completing the modification stage and producing

the final emulsified bio-asphalt, as shown in Fig. 6.

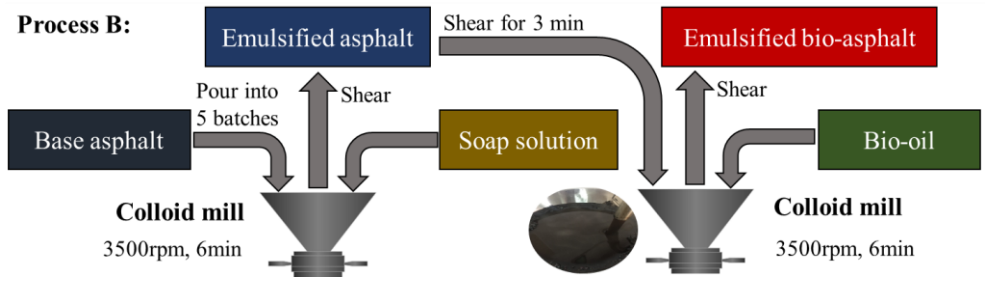

Fig. 6. Preparation process B: Emulsification followed by modification

(3) Process C: Separate emulsification followed by mixing

In Process C, we leverage the direct emulsification capability of bio-oil. Both the emulsified asphalt and emulsified bio-oil are prepared separately under same conditions and are then combined in a mixer at ambient temperature, specifically at 25°C, as shown in Fig. 7. The components are mixed at a rotational speed of 2000rpm for 10 minutes to form the final emulsified bio-asphalt.

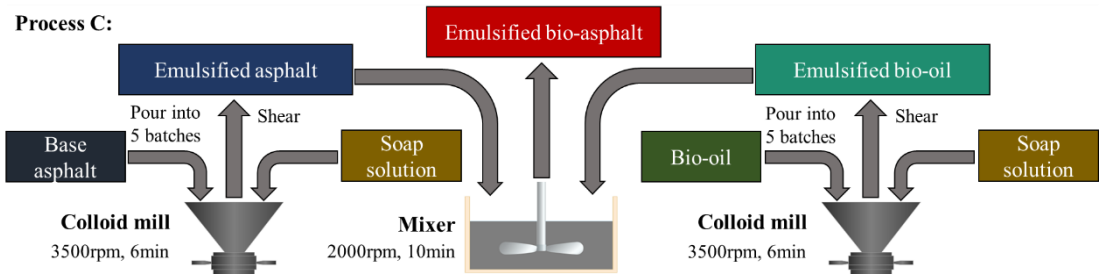

Fig. 7. Preparation process C: Separate emulsification followed by mixing

2.4 I-optimal experimental design

I-optimal method is a design approach aimed to enhance the precision and reliability of model parameters in experimental design. It can be combined with response surface methodology (RSM) to determine the optimal material compositions that meet specific performance requirements [34-36]. In this study, the I-optimal experimental model was designed using Design Expert 12.0.6 software, with control variables including bio-oil content, emulsifier content, and preparation process. Following previous research [29], this study applied relatively broad constraints on the proportions of control variables, as shown in Table 3. Bio-oil content and emulsifier content were set as continuous numerical variables, ranging from 0% to 30% and 0.5% to 5%, respectively. The preparation process was categorized as discrete

variables labeled A, B, and C, consistent with Section 2.3.

Table 3 Constraints for varying proportions of control variables

Control variables	Factors	Type	Level of variables	
			Low	High
Bio-oil	Numeric	Continuous	0	30%
Emulsifier	Numeric	Continuous	0.5%	5%
Preparation Process	Categoric	Discrete	Process A, Process B, Process C	

Table 4 presents the experimental design using I-optimal approach, consisting of 22 experimental groups. The spatial distribution of these groups is visually depicted in Fig. 8. To minimize experimental uncertainties, five sets of repetition points were introduced within the design. These points are identified as follows: Run #1 = #10 (Interior), Run #2 = #20 (Interior), Run #5 = #18 (Interior), Run #11 = #14 (CentEdge), and Run #16 = #21 (Interior).

Table 4 Experimental design of emulsified bio-asphalt using I-optimal approach

Run	Base Asphalt (%)	Bio-oil (%)	Emulsifier (%)	Preparation	Build type
1	100.00	23.55	4.01	Process A	Model
2	100.00	6.30	4.06	Process B	Replicate
3	100.00	0.00	0.50	Process B	Model
4	100.00	0.00	0.50	Process C	Lack of Fit
5	100.00	23.55	1.49	Process B	Model
6	100.00	30.00	2.75	Process C	Model
7	100.00	0.00	5.00	Process A	Model
8	100.00	0.00	5.00	Process C	Lack of Fit
9	100.00	0.00	2.75	Process C	Model
10	100.00	23.55	4.01	Process A	Replicate
11	100.00	15.00	0.50	Process C	Replicate
12	100.00	15.00	5.00	Process C	Model
13	100.00	30.00	0.50	Process A	Model
14	100.00	15.00	0.50	Process C	Model
15	100.00	30.00	5.00	Process B	Model
16	100.00	6.45	1.45	Process A	Replicate
17	100.00	9.90	1.99	Process B	Lack of Fit
18	100.00	23.55	1.49	Process B	Replicate
19	100.00	19.80	3.52	Process B	Lack of Fit
20	100.00	6.30	4.06	Process B	Model
21	100.00	6.45	1.45	Process A	Model
22	100.00	30.00	5.00	Process C	Lack of Fit

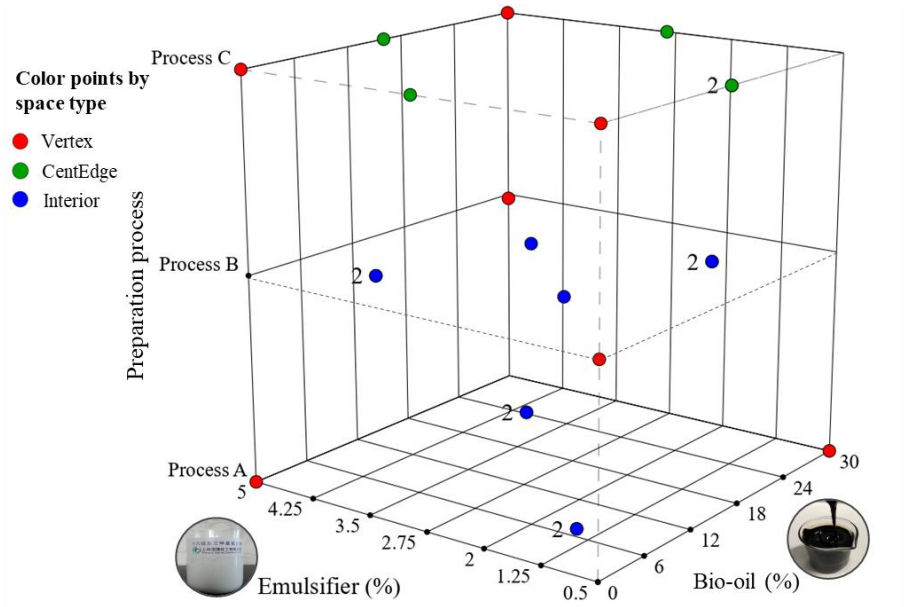

Note: Process A: modification followed by emulsification; Process B: emulsification followed by modification; Process C: separate emulsification and mixing; "2" in the figure represents "repetition point".

Fig. 8. The distribution of experimental points within the design space

To confirm the effectiveness of the I-optimal model, a comparative analysis was conducted with three alternative experimental design methods, namely A-optimal, D-optimal, and modified distance optimal. This comparison considered the mean standard error and the fraction of design space (FDS) values within an 95% confidence level. As shown in Fig. 9, the I-optimal model exhibited the lowest mean standard error value of 0.855 within the design space, indicating its superior predictive accuracy compared to the other methods. This can be attributed to the design principle of I-optimal model, which aims to minimize the prediction variance and allows it to effectively capture complex non-linear relationships between factors and responses [37]. In contrast, A-optimal, D-optimal, and modified distance optimal methods emphasize different design objectives, such as maximizing model accuracy, minimizing parameter bias, or achieving even distribution of points within the design space. Although these alternatives have their benefits in specific scenarios, they cannot prioritize the reduction of prediction variance as effectively as the I-optimal model [38]. Moreover, the I-optimal method also exhibits stability when dealing with a combination of continuous and categorical factors [39].

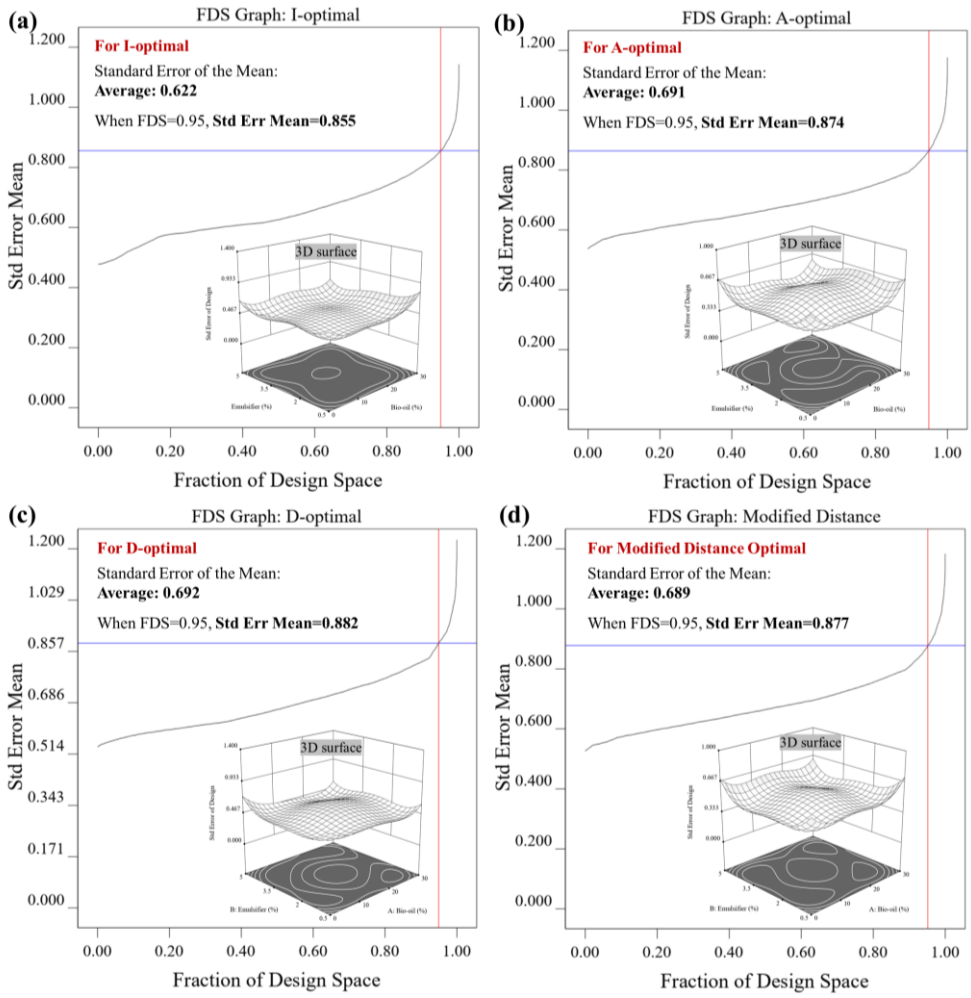

Fig. 9. Comparison of fraction of design space using different experimental design methods: (a) I-optimal; (b) A-optimal; (c) D-optimal; (d) Modified distance optimal

2.5 Performance testing metrics

This study conducted a comprehensive assessment of the emulsion performance and the residual's road performance of emulsified bio-asphalt. Emulsion performance was evaluated by measuring the medium particle size, specific surface area, and 5-day storage stability. The road performance of evaporation residues primarily included penetration, softening point, ductility, and the interfacial adhesion strength with aggregates. These performance metrics serve as response variables in the RSM model, with the detailed testing methods outlined in Section 3.

2.6 Desirability optimization methodology (DOM)

The desirability optimization methodology (DOM) is a statistical-based approach for multi-objective optimization. It is used to determine the optimal or near-optimal conditions of control variables that leads to desired values of response variables [40,

41]. Desirability serves as an objective function, ranging from 0 (indicating configurations where all responses are unacceptable) to 1 (representing the achievement of all desired responses). The simultaneous objective function *D* is the geometric mean of the desirability values for each response and is calculated using Equation (1).

$$D = (d_1 \cdot d_2 \cdot \ldots \cdot d_n)^{\frac{1}{n}} = (\prod_{i=1}^{n} d_i)^{\frac{1}{n}} \quad (1)$$

Where *D* represents the simultaneous desirability function; d_i is the desirability values for each response; *n* is the total number of responses, which is 7 in this case. For simultaneous optimization, every goal must be assigned a low and high value.

When the goal is to search for maximum responses, the desirability d_i is calculated using Equation (2).

$$\begin{cases} d_i = 0, \text{ if response} < \text{low value} \\ 0 < d_i < 1, \text{as response varies from low to high} \\ d_i = 1, \text{ if response} > \text{high value} \end{cases} \quad (2)$$

When the goal is to search for minimum responses, the desirability d_i is calculated using Equation (3).

$$\begin{cases} d_i = 1, \text{ if response} < \text{low value} \\ 1 > d_i > 0, \text{as response varies from low to high} \\ d_i = 0, \text{ if response} > \text{high value} \end{cases} \quad (3)$$

3. Test methods

Table 5 presents the evaluation metrics for emulsion performance and residual's road performance, along with their corresponding reference standards. Each of these tests was conducted three times, and the mean of these triplicates was taken as the final value for each response variable.

Table 5 Performance testing metrics for emulsified bio-asphalt

Type	Testing item	Units	Reference standard
Emulsion performance	Medium particle size	μm	ASTM E799
	Specific surface area	m^2/kg	
	5d storage stability	%	ASTM D244

Acquisition of evaporation residues			AASHTO PP72
Residues' road performance	Penetration	0.1mm	ASTM D5
	Softening point	℃	ASTM D36
	Ductility at 10℃	cm	ASTM D113
	Interfacial adhesion strength	MPa	ASTM D4541

3.1 Emulsion performance

In this study, the evaluation of emulsion performance involves conducting tests on droplet size distribution and storage stability, which reflect the uniformity and stability of emulsified bio-asphalt during the construction process.

3.1.1 Droplet size distribution test

In oil-in-water (O/W) emulsions, oil-phase particles (bio-asphalt) are dispersed within the water phase. The droplet size distribution of the emulsified bio-asphalt was characterized using a laser particle size analyzer (LPSA), specifically the Malvern Mastersizer 3000 model. Prior to testing, the emulsified bio-asphalt specimen was thoroughly mixed and placed in a chamber to prevent sedimentation or phase separation. During testing, a laser was directed onto the droplets within the specimen, and variations in scattered light intensity and angle were used to obtain information about the droplet size distribution. The medium particle size (D50) and specific surface area were chosen as the evaluation metrics. Generally, emulsions with smaller particle sizes and larger specific surface areas tend to exhibit better stability.

3.1.2 Storage stability test

The 5-day storage stability of emulsified bio-asphalt was evaluated using SYD-0655 glass test tubes. The effective height of the test tube is 310 mm, with a volume of 250 ml and an internal diameter of 32 mm. Prior to testing, the emulsified bio-asphalt was filtered through a 1.18 mm sieve, and then poured into the test tube up to the 250 ml mark. The sealed tubes were placed on a rack at 25℃ for a duration of 5 days. After the settling period, 50 g specimens were collected from the upper and lower ports of the tube, and their solids content was tested according to the EN 13074 standard. The 5-day storage stability can be calculated using Equation (4).

$$S_{5d} = \left| P_A - P_B \right| \times 100\% \tag{4}$$

Where S_{5d} represents the 5-day storage stability of emulsified bio-asphalt, %; P_A

is the solids content of the specimen collected from the upper port, g; P_B is the solids content of the specimen collected from the lower port, g.

3.2 Evaporation residue performance

To accurately simulate the actual moisture evaporation in emulsion, the low-temperature evaporation method according to AASHTO PP72 was employed to obtain the evaporation residues of emulsified bio-asphalt. Initially, the emulsion was evenly applied on square silicone pads at a rate of 2.0 kg/m² and left to evaporate for 24 hours at 25°C. This step aimed to facilitate emulsion evaporation at room temperature while preventing the formation of a skin on the surface. Subsequently, the coated pads were exposed to 60°C in a well-ventilated oven for 24 hours, yielding the evaporation residues. The road performance of residues was evaluated using the following metrics: penetration, softening point, ductility at 10°C, and the interfacial adhesion strength with aggregates.

3.2.1 Penetration test

The HDLZ-IV automatic penetration tester was used to measure the penetration of evaporation residues from emulsified bio-asphalt. Penetration refers to the depth, measured in units of 0.1mm, to which a standard 100g needle penetrates an asphalt specimen within a 5-second timeframe at 20°C. Generally, a higher penetration value indicates a softer asphalt texture and lower viscosity.

3.2.2 Softening point test

The HDLR-IV automatic tester was used to measure the softening point, which is valuable for evaluating the high-temperature stability of emulsified bio-asphalt. During the test, the specimen was placed within a copper ring with a diameter of 16mm and a height of 6mm. A standard steel ball was placed on the specimen, and the assembly was then immersed in water. The temperature was raised at a rate of 5℃/min. The softening point corresponds to the temperature at which the asphalt binder softens and descends to contact the lower plate surface.

3.2.3 Ductility test

The ductility at 10°C of evaporation residues from emulsified bio-asphalt was measured using an HDLY-V digital dual-speed ductility tester, with a pulling rate of 1

cm/min. A higher ductility value indicates better low-temperature extensibility of the asphalt binder, while a lower value suggest potential for cracking and brittle failure in low-temperature conditions.

3.2.4 Interfacial adhesion test

According to the ASTM D4541-17 standard, a modification was made to measure the adhesion between asphalt binder and aggregates using a UTM-30 servo hydraulic tester coupled with a self-developed fixture, as shown in Fig. 10. Initially, limestone aggregates, hailing from Jingyang, Shaanxi, were crafted into cylinders with a diameter of 25mm and a height of 15mm, each exhibiting a smooth polished surface. The selected limestone demonstrated an apparent relative density of 2.685 g/cm³ and a water absorption rate of 1.25%, with a mineral composition comprising 97.6% calcite, 1.4% dolomite, 0.5% siderite, and 0.5% other minerals. Molten asphalt binder was evenly applied to one aggregate surface, followed by covering it with another aggregate of identical specifications, forming a sandwiched specimen. The asphalt binder film thickness was controlled at 100μm ± 5μm through measurements at five different positions using a digital caliper. Before testing, the specimens were kept in a temperature-controlled chamber at 5℃ for 4 hours. Subsequently, these sandwiched specimens were placed in the self-developed fixture, with a pull head connected to an extended rod of the UTM-30 equipment. The loading rate was set at 1mm/min, and load-displacement curves were recorded. The occurrence of a distinct inflection point in the curve indicated the attainment of a critical tension threshold, signifying interfacial adhesion failure. This point, referred to as the "break point," was used to calculate the interfacial adhesion strength σ_a using Equation (5).

$$\sigma_a = F/A \tag{5}$$

Where σ_a represents the interfacial adhesion strength, MPa; F is the maximum load value on the load-displacement curve, N; and A is the cross-sectional area of the cylindrical aggregates, mm².

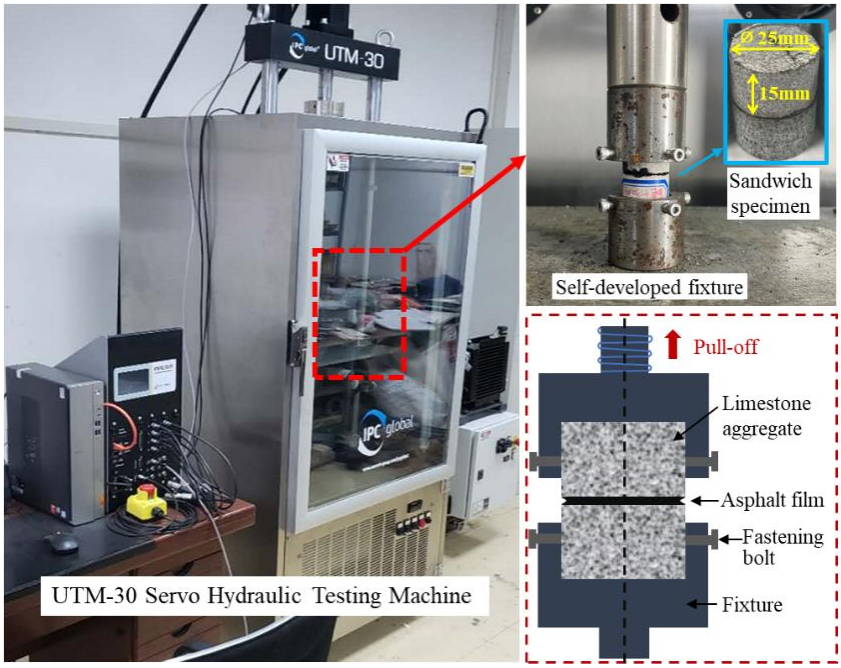

Fig. 10. Testing method for interfacial adhesion strength between asphalt binder and aggregates

3.3 Fourier Transform Infrared Spectroscopy (FTIR) analysis

The chemical composition and functional groups of the 90# base asphalt binder and bio-oil were identified using an FTIR analysis conducted on a Nicolet IS 50/6700 FTIR spectrometer. Samples were prepared by mixing with potassium bromide (KBr) and compressing into discs. Spectra were recorded in the range of 4000 cm^{-1} to 400 cm^{-1}, with an accumulation of 32 scans per sample to ensure clarity and reproducibility of the data.

4. Results and discussion

Table 6 summarizes the test results for the emulsion and residue performance of emulsified bio-asphalt, serving as the foundation for constructing the response surface model. Table 7 presents the ANOVA results from fitting models for each response variable. It is evident that the test results for each performance indicator can be well-fitted by the quadratic model, with high correlation coefficients ($R^2 > 0.95$) and considerable significance levels (P-value<0.0001). Additionally, the Adj-R^2 values consistently exceed 0.9, indicating the model keeps good fitting capability when accounting for the loss of degrees of freedom. Moreover, the Pred-R^2 values are also maintained at a high level (above 0.8), indicating the fitting model not only explains the relationship between control factors and response variables but also exhibits the

capacity to accurately predict outcomes beyond the scope of the training data.

Table 6 Test results for emulsion and residue performance of emulsified bio-asphalt

Run	Emulsion performance			Residue's road performance			
	Medium particle size (μm)	Specific surface area (m^2/kg)	5d storage stability (%)	Penetration (0.1mm)	Softening point (℃)	Ductility at 10℃ (cm)	Interfacial adhesion strength (MPa)
1	3.3	904	2.23	102	44.3	69.5	0.733
2	4.7	703	3.94	101	45.1	54.3	0.661
3	5.3	665	4.59	93	45.7	42.9	0.616
4	4.8	869	3.28	91	46.2	44.8	0.638
5	5.7	687	4.96	111	41.2	69.6	0.691
6	3.5	915	2.84	112	42.2	75.6	0.819
7	3.7	890	1.81	96	46.6	45.2	0.669
8	3.9	871	2.25	96	46.0	60.4	0.668
9	3.9	911	2.02	98	46.1	62.7	0.707
10	3.2	905	2.46	104	44.5	70.4	0.728
11	4.6	872	3.90	95	44.8	66.0	0.820
12	3.8	909	2.78	103	44.5	69.8	0.822
13	4.1	880	4.20	101	44.0	62.3	0.687
14	4.5	875	3.87	98	44.7	66.8	0.815
15	5.5	689	4.14	112	39.5	66.6	0.659
16	3.8	885	2.65	98	46.5	53.0	0.702
17	5.0	705	4.39	107	44.7	63.1	0.695
18	5.6	692	5.20	113	41.2	70.0	0.693
19	5.1	699	3.92	108	42.7	76.5	0.706
20	4.8	703	3.83	102	45.0	53.8	0.658
21	3.7	890	2.68	97	46.5	54.9	0.710
22	3.6	912	3.09	107	42.0	72.1	0.790

Table 7 Model fit and ANOVA results of each response variable

Response variables	Fitting model	R^2	Adj-R^2	Pred-R^2	F-value	P-value
Medium particle size	Quadratic model	0.9958	0.9912	0.9576	215.34	<0.0001
Specific surface area		0.9965	0.9926	0.9287	257.04	
5-day storage stability		0.9866	0.9718	0.8957	66.78	
Penetration		0.9702	0.9375	0.8511	29.62	
Softening point		0.9953	0.9902	0.9377	193.27	
Ductility at 10℃		0.9539	0.9033	0.8611	179.53	
Interfacial adhesion strength		0.9662	0.9291	0.8229	26.02	

4.1 Emulsion performance

Fig. 11 is the contour plots of emulsion performance generated by a quadratic model, revealing the influence of preparation processes and component content on medium particle size, specific surface area, and 5-day storage stability.

As shown in Fig. 11 (a)-(c), emulsified bio-asphalt prepared via Process A exhibits the smallest medium droplet size, ranging from 3.2μm to 4.2μm. Process C follows, while emulsion droplet particles from Process B maintain higher values, exceeding 4.6μm. The test results of specific surface area for emulsion droplets are

presented in Fig. 11 (d)-(f). Generally, smaller particle sizes correspond to larger specific surface areas, and this trend is supported by the findings of this study. Emulsified bio-asphalt from both Process A and C have specific surface areas exceeding 870m²/kg, while those from Process B exhibit specific surface areas mostly below 700m²/kg. For Process A and C, the increase of bio-oil content leads to a slight reduction in emulsion particle size. This can be attributed to the relatively smaller molecular structure of bio-oil, which makes it more susceptible to shear forces during the emulsification process, resulting in its dispersion into smaller droplets. In contrast, the increase of bio-oil content in Process B leads to an enlargement of emulsion particle size, possibly due to insufficient emulsification of the bio-oil. A consistent observation is that emulsion particle size is minimized and specific surface area is maximized when the emulsifier content falls within the approximate range of 3.2% to 3.5%.

Fig. 11 (g)-(i) present the test results of 5-day storage stability for emulsified bio-asphalt. The order of S_{5d} values is as follows: Process A < Process C < Process B, indicating that emulsion prepared by Process A exhibits the best storage stability. In Process A (modification followed by emulsification), the bio-oil is initially mixed with the base asphalt binder at high temperatures, which make it easier to be uniformly dispersed in the subsequent emulsification process. The above procedure enhances the emulsion's ability to resist separation. In contrast, employing an emulsification followed by modification approach, as seen in Process B, may lead to insufficient interaction between bio-oil and emulsifier, which can cause significant variations in droplet dispersion and increase the likelihood of gravitational settling for larger-sized particles. Process C involves separate emulsification of bio-oil and base asphalt binder followed by mixing, and the overall emulsion performance aligns closely with that of Process A. Moreover, the addition of bio-oil negatively impacts the storage stability across all three preparation processes, and optimal storage stability is achieved when the emulsifier content is around 3.5%.

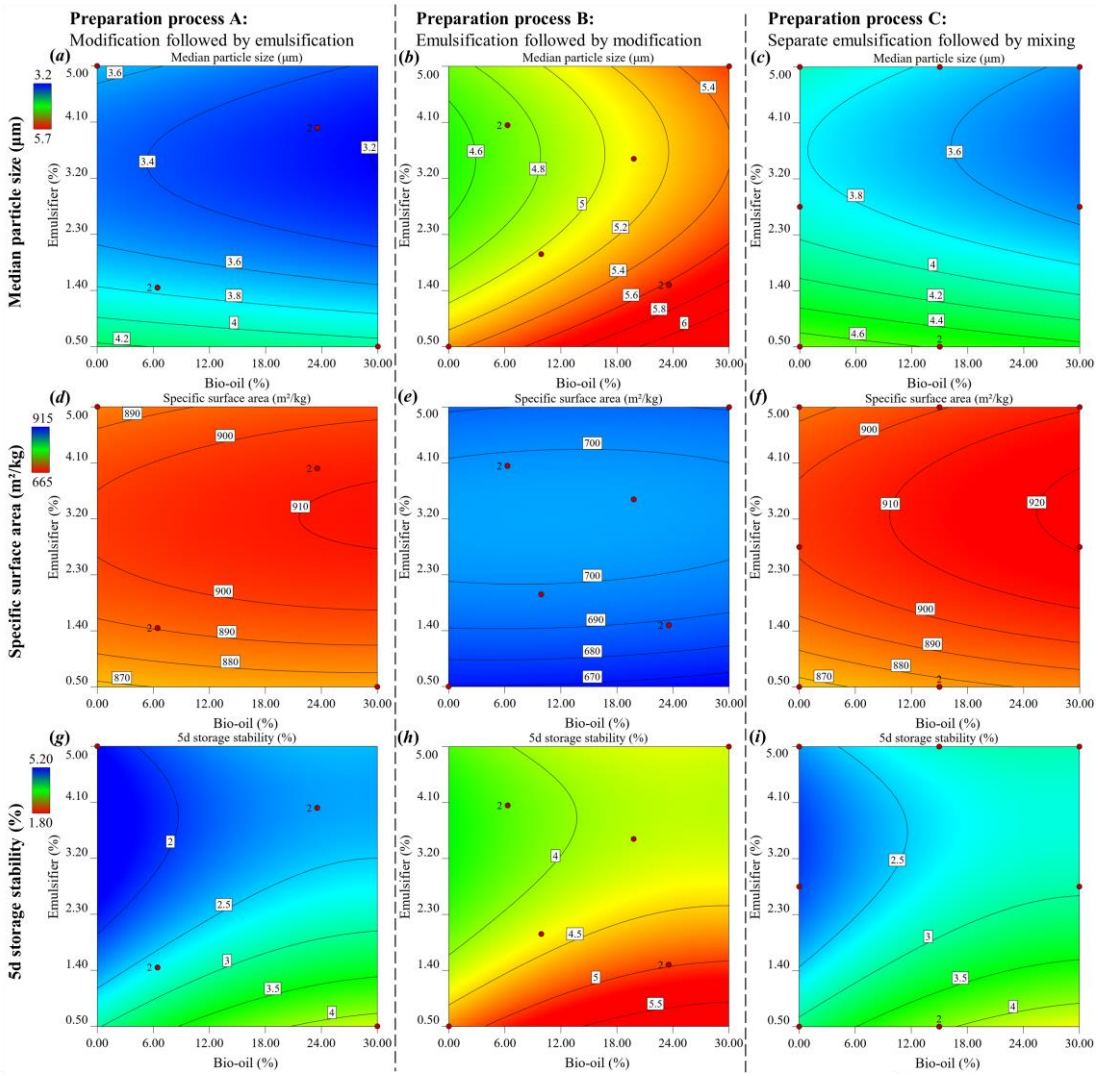

Fig. 11. Influence of preparation process and component content on emulsion performance: Contour plots

4.2 Evaporation residue performance

Fig. 12 shows the influence of preparation processes and component content on residue's road performance, including penetration, softening point, ductility at 10°C, and the interface adhesion strength with limestone aggregates.

In Fig. 12 (a)-(c), the penetration test results show that the residue of emulsified bio-asphalt prepared via Process A exhibits the lowest penetration value. This can be attributed to the modification followed by emulsification approach, where the bio-oil needs to be mixed with the base asphalt binder at 140°C, leading to the volatilization of lighter components and slight aging of the bio-oil. Similar trends are also evident in the test results of softening point (Fig. 12 d-f) and ductility at 10°C (Fig. 12 g-i). In Process A, the residue of emulsified bio-asphalt exhibits the highest softening point

and the lowest ductility value. Emulsified bio-asphalt prepared through Process B struggles to fully exploit the low-temperature flexibility advantages of bio-oil, resulting in relatively modest improvements in ductility. In contrast, owing to the favorable emulsion fusion resulting from the stepwise emulsification and mixing approach, Process C can leverage the low-temperature performance benefits of bio-oil and effectively avoids poor high-temperature performance of the hot-mix bio-asphalt binder.

A consistent observation is that increasing bio-oil content leads to higher penetration and ductility at 10°C of emulsified bio-asphalt residues, while reducing the softening point. As the emulsifier content increases, both the penetration and ductility at 10°C initially increase and then decrease, reaching a peak at around 3.2% emulsifier content. However, the influence of emulsifier on the softening point is limited. When the STAC emulsifier content is relatively low, it can effectively reduce the interfacial tension between the oil and water phases, promoting the emulsification of bio-oil and base asphalt binder. Nevertheless, when the emulsifier content exceeds a certain threshold, the unreacted emulsifier will remain in a free state within the soap solution, negatively affecting the high-temperature performance and extensibility of the emulsified bio-asphalt.

As shown in Fig. 12 (j)-(l), the emulsified bio-asphalt prepared by Process C exhibits the highest interfacial adhesion strength with limestone aggregates. This enhanced performance can be linked to the efficient dispersion of bio-oil within the emulsion facilitated by the stepwise emulsification and mixing approach of Process C. This claim is supported by the emulsion performance data, where Process C yields a smaller median droplet size and greater storage stability than Process B, indicating better dispersion of bio-oil. Additionally, evaporation residue performance tests reveal that Process C maintains bio-oil's inherent properties more effectively than Process A, evidenced by higher penetration, lower softening points, and greater ductility in Process C. Upon the addition of bio-oil, the specimen shows enhanced affinity and adhesion to alkaline aggregates [42], but the bio-oil content should be maintained within a reasonable range. In the case of Process C, the value of interface adhesion

strength reaches a peak when bio-oil content is 23%. Moreover, the addition of emulsifiers also enhances the adhesion effect, with the most significant improvement observed at an emulsifier content of approximately 3%.

The improved adhesion by bio-oil can be attributed to its chemical properties. A comparative analysis of functional groups and compound compositions between 90# base asphalt binder and bio-oil was conducted using FTIR spectroscopy, as shown in Table 8. The infrared spectral features of bio-oil almost encompass all the characteristic peaks of the base asphalt binder, primarily composed of aromatic compounds, aliphatic compounds, sulphoxides, and other atomic derivatives. However, bio-oil exhibits three distinct peaks in the absorbance spectrum at 1692, 1273, and 1109 cm^{-1}, corresponding to the C=O and C–O segments of esters. The addition of ester-containing bio-oil into base asphalt binder increases the polar portion (sum of resin and asphaltenes), thereby enhancing its interfacial adhesion with alkaline aggregates [43]. Furthermore, the concentrated peaks at 3306 cm^{-1} in the spectrum indicate that the bio-oil has a complex composition containing alcohols, liquid water, and nitrogenous compounds, which underscores the existing challenges in terms of bio-oil stability [44].

Table 8 FTIR analysis of functional groups of 90# base asphalt binder and bio-oil

Material	Absorption (cm^{-1})	Group	Compound class
90# base asphalt	757	C-H bending	Aromatic compounds
	1031	S=O stretching	Sulphoxide
	1377 and 1454	-CH_3 stretching	Aliphatic compounds
	1601	C=C stretching	Aromatic compounds
	2844 and 2918	C-H stretching	Alkanes
Bio-oil	757	C-H bending	Aromatic compounds
	1031	S=O stretching	Sulphoxide
	1109 and 1273	C-O stretching	Esters and phenols
	1377 and 1454	-CH_3 stretching	Aliphatic compounds
	1509	N-O stretching	Nitrosamines
	1601	C=C stretching	Aromatic compounds
	1692	C=O stretching	Esters, ketones and aldehydes
	2844 and 2918	C-H stretching	Alkanes
	3306	N-H stretching O-H stretching	Alcohols, liquid water and nitrogenous compounds

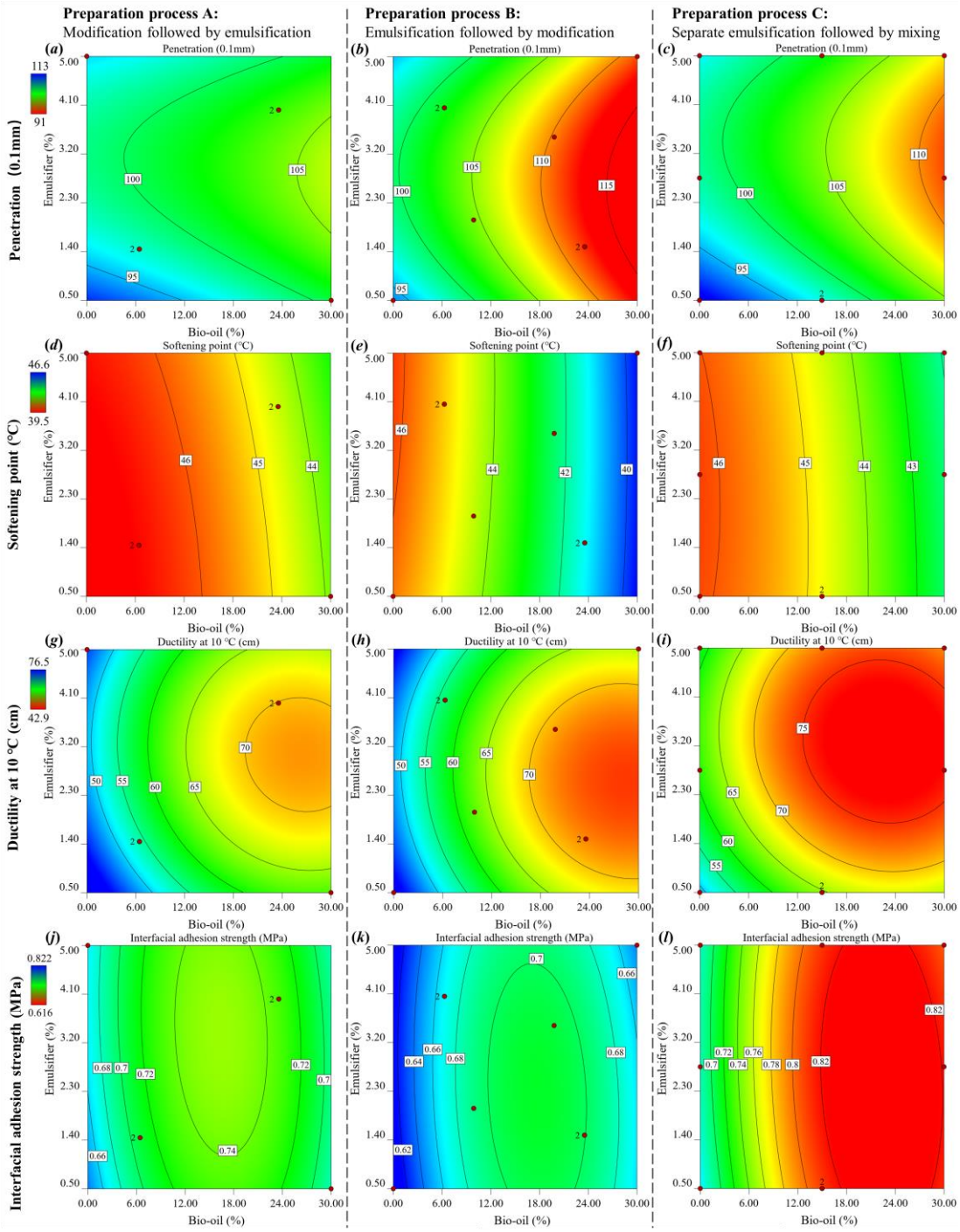

Fig. 12. Influence of preparation process and component content on residue's road performance: Contour plots

4.3 Multi-objective optimization

Table 9 summarizes the overall influence trends of preparation processes and component contents on the response variables. It defines optimization goals for various performance indicators. The objective of this study is to identify an emulsified bio-asphalt production method that balances both emulsion performance and residue's road performance. Specifically, this balance aims to ensure uniform emulsion

dispersion and stable storage, while also possessing favorable high-temperature stability, low-temperature extensibility, and good interfacial adhesion capability with aggregates.

Table 9 Overall influence trends of factors on responses and the optimization goals

Response variables	Influence of preparation process	Variation with increasing bio-oil content	Variation with increasing emulsifier content	Goal
Medium particle size	Process A < C < B	For processes A and C: decrease. For process B: increase.	Decrease initially, then increase.	Minimize
Specific surface area	Process C≈A > B	For processes A and C: increase slightly. For process B: decrease.	Increase initially, then decrease.	Maximize
5d storage stability	Process A < C < B	Increase	Decrease initially, then increase.	Minimize
Penetration	Process A < C < B	Increase	Increase initially, then decrease.	Minimize
Softening point	Process A > C > B	Decrease	Decrease slightly.	Maximize
Ductility at 10℃	Process C > A≈B	Increase	Increase initially, then decrease.	Maximize
Interfacial adhesion strength	Process C > A > B	Increase initially, then decrease.	Increase initially, then decrease.	Maximize

According to Section 2.6, the core principle of desirability optimization methodology (DOM) involves integrating the simultaneous desirability function (*D*) with the response surface methodology (RSM) to achieve multi-objective optimization. Fig. 13 shows the desirability distribution contour and the influence trend of single factors, visualizing changes in desirability values using color gradients. The cool blue color represents lower desirability value, while the warm green color indicates higher desirability value. It is evident that for each preparation process, there exists a specific design point with the highest desirability value. The optimal content of bio-oil and emulsifier corresponding to this point can be identified from the chart depicting the influence of single factors.

In this study, equal weighting was assigned to each performance indicator within the DOM framework, aiming for a holistic optimization of the emulsified bio-asphalt composition. Nevertheless, the inherent versatility of the DOM permits the modification of these weights to prioritize certain indicators over others. This adaptability is particularly beneficial for tailoring emulsion formulations to meet specific end-use conditions, whether prioritizing workability for ease of application or durability for long-term road performance. Future research will delve into optimizing

these weights for targeted asphalt emulsion properties.

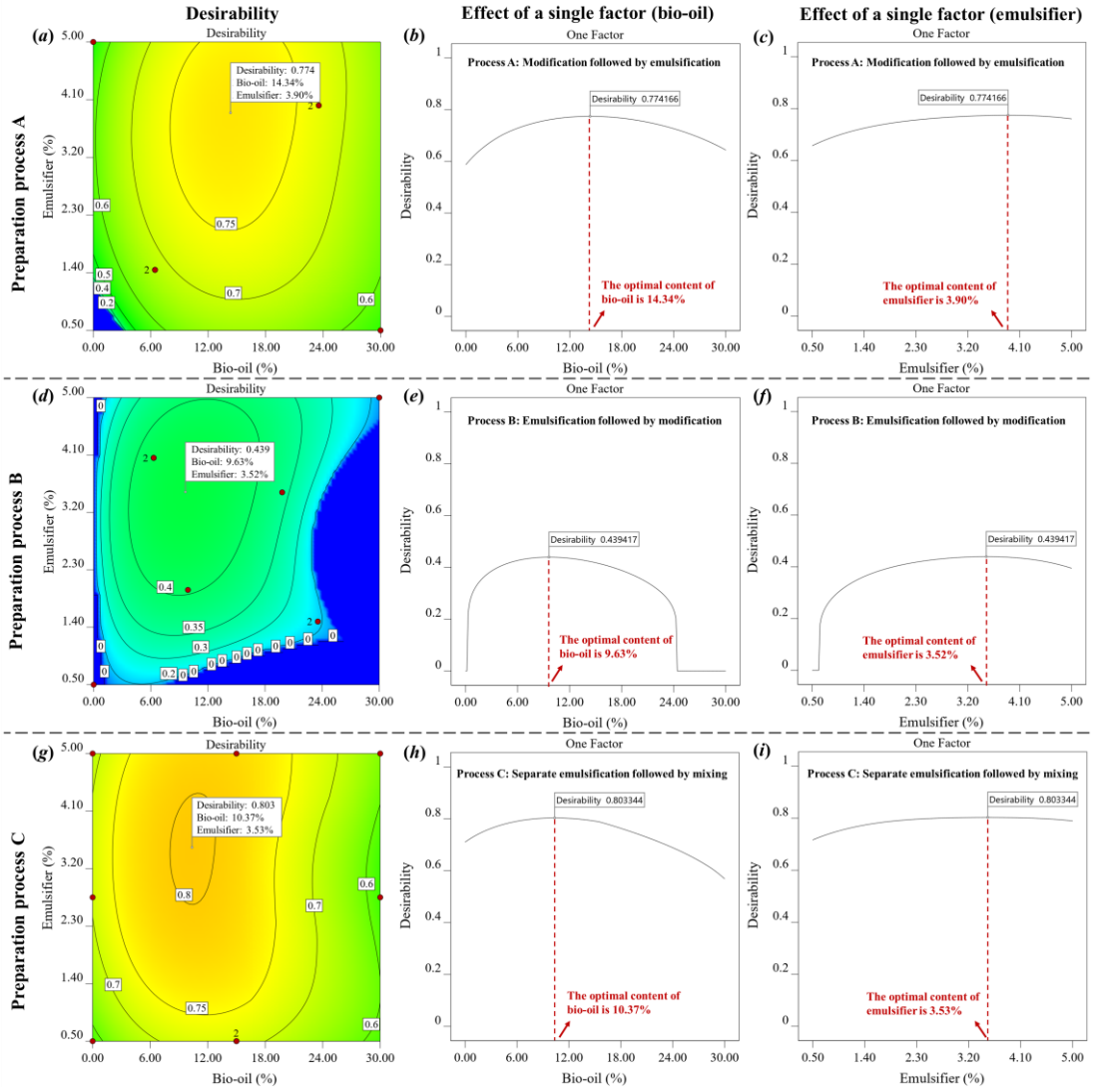

Fig. 13. Desirability distribution contour and the influence trend of single factors

Table 10 provides the solutions with the highest desirability values among the three preparation processes. The predictive accuracy is verified through practical performance testing, which reveals that the differences between actual and predicted values for each response variable remain within acceptable ranges. These results strongly affirm the effectiveness of the optimization design approach using DOM. The solution corresponding to Process C exhibits the highest desirability value of 0.803, with an optimal composition of 10.37% bio-oil and 3.53% emulsifier.

Table 10 Optimal solutions for each preparation process using DOM method

Optimal solutions for each preparation process	**Process A:** 14.34% bio-oil and 3.90% emulsifier	**Process B:** 9.63% bio-oil and 3.52% emulsifier	**Process C:** 10.37% bio-oil and 3.53% emulsifier

Desirability	0.774		0.439		0.803	
Medium particle size (μm)	Predicted	3.3	Predicted	4.8	Predicted	3.7
	Actual	3.5	Actual	5.2	Actual	3.6
Specific surface area (m^2/kg)	Predicted	905	Predicted	705	Predicted	910
	Actual	888	Actual	680	Actual	900
5-day storage stability (%)	Predicted	2.18	Predicted	3.90	Predicted	2.46
	Actual	2.35	Actual	3.83	Actual	2.50
Penetration (0.1mm)	Predicted	101	Predicted	104	Predicted	103
	Actual	101	Actual	99	Actual	104
Softening point (℃)	Predicted	45.7	Predicted	44.5	Predicted	45.3
	Actual	45.0	Actual	43.1	Actual	45.4
Ductility at 10℃ (cm)	Predicted	66.1	Predicted	62.2	Predicted	73.3
	Actual	65.5	Actual	61.0	Actual	72.3
Interfacial adhesion strength (MPa)	Predicted	0.748	Predicted	0.690	Predicted	0.793
	Actual	0.736	Actual	0.675	Actual	0.790

5. Environmental and Economic Benefits Assessment

This study proposes three preparation processes for emulsified bio-asphalt and presents component design solutions based on multi-objective performance optimization in Section 4. This section primarily investigates the practical environmental and economic benefits of emulsified bio-asphalt. The emission gas detection and cost estimation were conducted with the assistance of the asphalt heating tank and emulsification plant (mainly referring to the colloid mill) provided by Shaanxi Highway Mechanization Co., Ltd. The selection of raw materials such as base asphalt binder, bio-oil, and emulsifier remain consistent with the experimental research previously described in this paper.

5.1 Environmental benefits

Due to the varying sequences of asphalt modification and emulsification among the three proposed methods, the bio-oil undergoes different processing sequences and timings. This leads to varying environmental impacts during the production of emulsified bio-asphalt. As depicted in Fig. 14, emissions were primarily monitored from the asphalt tank during the heating and insulation phases, as well as from the asphalt emulsification process. The actual production conditions for emulsified bio-asphalt, including heating temperature, shear rate, emulsification temperature, and shear duration, align with the laboratory preparation conditions described in Section 2.3. The optimal bio-oil and emulsifier content as described in Section 4.3 was

adopted for the three production processes. Following standards set by the U.S. Environmental Protection Agency (EPA), the collected emissions were analyzed for concentrations of carbon dioxide (CO_2), sulfur dioxide (SO_2), volatile organic compounds (VOCs), carbon monoxide (CO), and nitrogen oxides (NOx), measured in ppmv (parts per million by volume).

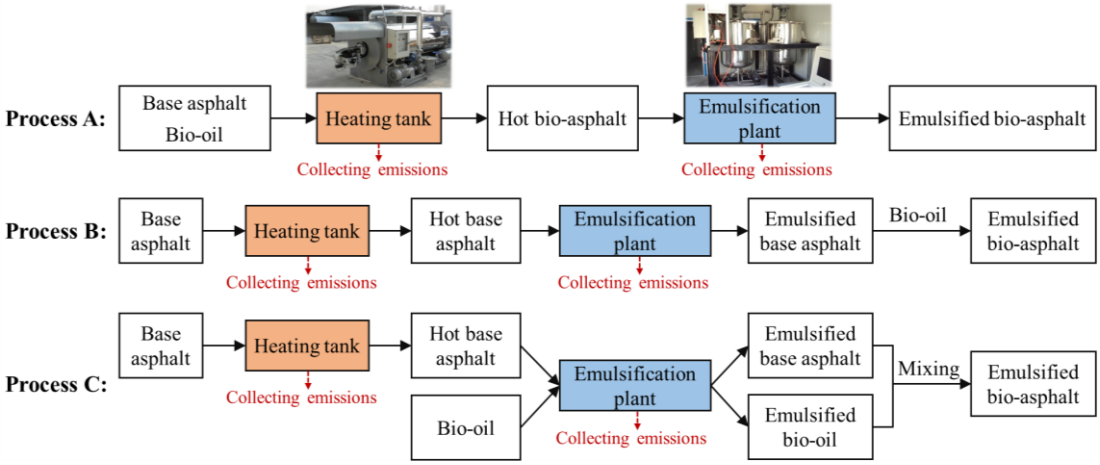

Fig. 14. Emissions collection from asphalt heating and emulsification processes in three emulsified bio-asphalt production methods

Fig. 15 presents the concentrations of greenhouse and harmful gas emissions measured during the production of emulsified bio-asphalt. In the asphalt heating phase, Process A's method of preheating and mixing the bio-oil with base asphalt binder led to higher CO_2 and harmful gas emissions compared to Processes B and C, which adopted a strategy of adding bio-oil solely during the emulsification phase. Referring to Table 8, the bio-oil, enriched with light components like various aromatic compounds, tends to release higher levels of NOx and VOCs when mixed with asphalt binder at high temperatures [10, 45]. In contrast, emulsification stage significantly reduces both greenhouse and harmful gas emissions, offering an advantage not observed in traditional hot-mix asphalt binder. Using Process C, bio-oil and base asphalt binder are emulsified separately and then combined at room temperature. This method can precisely control the emulsification temperature conditions to minimize the volatilization of VOCs and NOx, achieving superior environmental benefits.

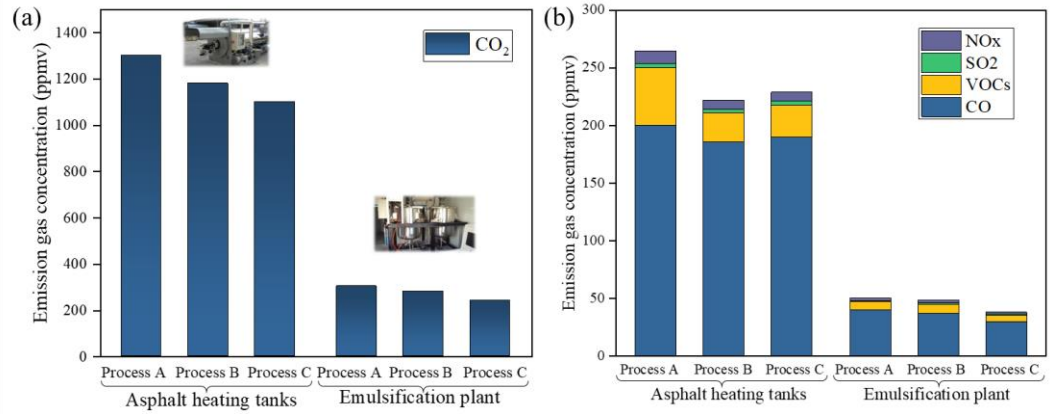

Fig. 15. Greenhouse gas and harmful gas emissions during the production of emulsified bio-asphalt

In essence, utilizing bio-oil as a substitute for petroleum-based asphalt binder represents a zero-carbon construction approach [6]. Bio-oil contains a substantial amount of carbon, with the pyrolyzed bio-oil from wood chips in this study exceeding 55% carbon content. Plants initially absorb CO_2 through photosynthesis and transform it into biomass, which is then converted to bio-oil via solvent extraction and thermochemical processes. Bio-oil is considered carbon-neutral since the CO_2 uptake by plants offsets the CO_2 emissions during its production [7]. Consequently, employing bio-oil in road construction can be perceived as a potent carbon sequestration technique, preventing the carbon stored by plants from being released as CO_2 or methane upon natural decay or decomposition.

According to the United Nations Environment Programme (UNEP), there is a global commitment to achieve carbon neutrality by 2050, necessitating a 50% reduction in CO_2 emissions [46]. The transportation sector, represented by roads, stands as a primary contributor to carbon emissions [47], underscoring the critical challenge of energy conservation and carbon reduction. The bio-oil used in this study contains 55.6% non-fossil carbon (neutral carbon produced from CO_2 consumed by plants through photosynthesis), providing a promising avenue for carbon sequestration. Incorporating 10wt% bio-oil into the asphalt binder equates to a reduction of approximately 55 kg of carbon per ton of binder. Statistics show that as of the end of 2022, China's annual demand for asphalt concrete for road construction reached 410 million tons, correlating to an asphalt binder demand of around 16

million tons [48]. Substituting 10w% of petroleum-based asphalt binder with bio-oil can potentially sequester about 880,000 tons of carbon annually. Given the aforementioned low-emission advantages, this study further reinforces the perspective that the proposed emulsification technique offers an environmentally-friendly high-value utilization pathway for bio-oil.

5.2 Economic benefits

To assess the economic benefits of the application of emulsified bio-asphalt, a cost analysis was conducted. The fast pyrolysis technique utilized in this study can transform 1 ton of waste wood chips into 180 kilograms of bio-oil, indicating a conversion rate of 18%. Drawing from the petroleum market data of October 2023, the production cost for each ton of bio-oil is approximately 60% of the selling price of petroleum-based asphalt binder. This suggests that replacing 10wt% of petroleum-based asphalt binder with bio-oil can reduce asphalt production costs by 4%. Given China's annual consumption of 16 million tons of road petroleum asphalt binder [48], the application of bio-asphalt binder can lead to savings exceeding 3 billion CNY. The price of petroleum asphalt binder is subject to fluctuations due to constraints in resource reserves and geopolitical factors. In contrast, bio-oil, being renewable, is likely to maintain relative price stability as the technology matures [49, 50]. Furthermore, the emulsification process showcases significant energy efficiency benefits. Compared to traditional hot-mix asphalt binder, the emulsified method reduces the preparation temperature by more than 60℃, paving the way for cost savings and decreased dependency on non-renewable energy resources.

It's also noteworthy that the “emulsification followed by modification” approach (Process B) occasionally results in insufficient bio-oil emulsification. This has resulted in blockages within the material transport pipelines during the emulsified bio-asphalt production cycle, negatively impacting conversion efficiency. In practical production, Process B should be either avoided or additional maintenance costs should be considered.

6. Conclusion

(1) The optimal emulsification temperature was determined to be 80±1℃ based on the thermal characteristics of bio-oil. Three preparation processes for emulsified bio-asphalt were proposed, including modification followed by emulsification (Process A), emulsification followed by modification (Process B), and separate emulsification followed by mixing (Process C). These methods provide diverse pathways to obtain stable bio-asphalt emulsion systems.

(2) The integration of I-optimal model with response surface methodology (RSM) was used to systematically investigate the influence of preparation processes and component contents on the performance of emulsified bio-asphalt. This approach effectively captured nonlinear relationships between factors and responses, exhibiting better predictive accuracy compared to other design methods.

(3) Emulsified bio-asphalt prepared via Processes A and C exhibited superior emulsion performance, with finer emulsion particle size, larger specific surface area, and better storage stability. In Processes A and C, adding bio-oil slightly decreased emulsion particle size, while in Process B, insufficient bio-oil emulsification led to larger particles. The optimal range for emulsifier content is approximately 3.2% to 3.5% to achieve the best improvement of emulsion performance.

(4) Process A exhibits the drawback of bio-oil aging at 140℃ during asphalt modification, while Process B struggles with ensuring uniform bio-oil dispersion within the emulsion. Process C can leverage the low-temperature extensibility and adhesion benefits of bio-oil and avoid poor high-temperature performance of the hot-mix bio-asphalt binder. The addition of bio-oil increased penetration and ductility but decreased the softening point of the residue. The presence of unreacted free emulsifier negatively impacted road performance, and its content needs to be maintained around 3%.

(5) The desirability optimization methodology (DOM) was employed for multi-objective optimization of emulsified bio-asphalt. By integrating RSM with the desirability function, it can identify the optimal solution with the highest desirability

value, achieving a balance between emulsion and residue's road performance. The recommended preparation process is separate emulsification followed by mixing (Process C), with an optimal composition of 10.37% bio-oil and 3.53% emulsifier.

(6) Emulsified bio-asphalt production, especially using Process C, significantly reduces environmental impacts by minimizing VOCs and NOx emissions. Adopting bio-oil as a carbon-neutral alternative to petroleum-based asphalt binder can lead to the sequestration of about 880,000 tons of carbon annually in China. Economically, implementing bio-asphalt offers substantial benefits, potentially saving over 3 billion CNY in road construction and maintenance costs, while also enhancing energy efficiency and reducing dependence on non-renewable energy resources.

This study proposed a multi-objective optimization approach for preparing high-performance and easily producible emulsified bio-asphalt, presenting a sustainable and high-value utilization pathway for bio-oil through emulsification. Nevertheless, it's worth noting the limitations of this study. On the one hand, this study focuses on small-scale laboratory experiments, without considering the influence of environmental factors, traffic loads, and construction conditions. On the other hand, the current optimization framework is limited to the selected components used in this study. Future research should expand the range of experimental factors that influence emulsified bio-asphalt performance and encompass a wider variety of raw materials, in order to establish a more comprehensive correlation between materials and their performance.

Acknowledgements

This research was supported by the National Natural Science Foundation of China (NSFC) (No. 52078048), and the National Key Research and Development Program of China (No. 2021YFB2601000).

Declaration of Competing Interest

None.

References

[1] Wei Y, Chen K, Kang J, et al. Policy and management of carbon peaking and carbon neutrality: A literature review[J]. Engineering, 2022, 14: 52-63.

[2] Jędrzejczak P, Collins M N, Jesionowski T, et al. The role of lignin and lignin-based materials in sustainable construction–a comprehensive review[J]. International Journal of Biological Macromolecules, 2021, 187: 624-650.

[3] Al-Sabaeei A M, Napiah M B, Sutanto M H, et al. A systematic review of bio-asphalt for flexible pavement applications: Coherent taxonomy, motivations, challenges and future directions[J]. Journal of cleaner production, 2020, 249: 119357.

[4] Lv S, Liu J, Peng X, et al. Laboratory experiments of various bio-asphalt on rheological and microscopic properties[J]. Journal of Cleaner Production, 2021, 320: 128770.

[5] He L, Tao M, Liu Z, et al. Biomass valorization toward sustainable asphalt pavements: Progress and prospects[J]. Waste Management, 2023, 165: 159-178.

[6] Pahlavan F, Lamanna A, Park K B, et al. Phenol-rich bio-oils as free-radical scavengers to hinder oxidative aging in asphalt binder[J]. Resources, Conservation and Recycling, 2022, 187: 106601.

[7] Fini E H, Kalberer E W, Shahbazi A, et al. Chemical characterization of biobinder from swine manure: Sustainable modifier for asphalt binder[J]. Journal of Materials in Civil Engineering, 2011, 23(11): 1506-1513.

[8] Inayat A, Ahmed A, Tariq R, et al. Techno-economical evaluation of bio-oil production via biomass fast pyrolysis process: a review[J]. Frontiers in Energy Research, 2022, 9: 770355.

[9] Yang L, Wang X C, Dai M, et al. Shifting from fossil-based economy to bio-based economy: Status quo, challenges, and prospects[J]. Energy, 2021, 228: 120533.

[10] Lehto J, Oasmaa A, Solantausta Y, et al. Review of fuel oil quality and combustion of fast pyrolysis bio-oils from lignocellulosic biomass[J]. Applied Energy, 2014, 116: 178-190.

[11] Peng X, Xie N, Xia C, et al. Laboratory evaluation of different bio-oil recycled aged asphalts: Conventional performances and microscopic characteristics[J]. Journal of Cleaner Production, 2023, 428: 139442.

[12] Wang H, Ma Z, Chen X, et al. Preparation process of bio-oil and bio-asphalt, their performance, and the application of bio-asphalt: A comprehensive review[J]. Journal of Traffic and Transportation Engineering (English Edition), 2020, 7(2): 137-151.

[13] Gao J, Wang H, Liu C, et al. High-temperature rheological behavior and fatigue performance of lignin modified asphalt binder[J]. Construction and Building Materials, 2020, 230: 117063.

[14] Yuan J, Lv S, Peng X, et al. Comprehensive Properties Evaluation of Modified Bio-Asphalt Mixture Based on Comparison Matrix[J]. Journal of Materials in Civil Engineering, 2024, 36(3): 04023616.

[15] Huang T, He H, Zhang P, et al. Laboratory investigation on performance and mechanism of polyphosphoric acid modified bio-asphalt[J]. Journal of Cleaner Production, 2022, 333: 130104.

[16] Sun D, Sun G, Du Y, et al. Evaluation of optimized bio-asphalt containing high content waste cooking oil residues[J]. Fuel, 2017, 202: 529-540.

[17] Zhang R, Wang H, Gao J, et al. High temperature performance of SBS modified bio-asphalt[J]. Construction and Building Materials, 2017, 144: 99-105.

[18] Al-Sabaeei A M, Napiah M, Sutanto M, et al. Physicochemical, rheological and microstructural properties of Nano-Silica modified Bio-Asphalt[J]. Construction and Building Materials, 2021, 297: 123772.
[19] Koenders B G, Stoker D A, Bowen C, et al. Innovative process in asphalt production and application to obtain lower operating temperatures[C]//The 2nd Eurasphalt & Eurobitumen Congress, Barcelona, Spain. 2000: 830-840.
[20] Mercado R A, Salager J L, Sadtler V, et al. Breaking of a cationic amine oil-in-water emulsion by pH increasing: Rheological monitoring to modelize asphalt emulsion rupture[J]. Colloids and Surfaces A: Physicochemical and Engineering Aspects, 2014, 458: 63-68.
[21] Umar A A, Saaid I B M, Sulaimon A A, et al. A review of petroleum emulsions and recent progress on water-in-crude oil emulsions stabilized by natural surfactants and solids[J]. Journal of Petroleum Science and Engineering, 2018, 165: 673-690.
[22] Shanbara H K, Dulaimi A, Al-Mansoori T, et al. The future of eco-friendly cold mix asphalt[J]. Renewable and Sustainable Energy Reviews, 2021, 149: 111318.
[23] Ronald M, Luis F P. Asphalt emulsions formulation: State-of-the-art and dependency of formulation on emulsions properties[J]. Construction and Building Materials, 2016, 123: 162-173.
[24] Ouyang J, Meng Y, Tang T, et al. Characterization of the drying behaviour of asphalt emulsion[J]. Construction and Building Materials, 2021, 274: 122090.
[25] Chen C, Lin L, Ma T. Effects of Oil/Asphalt Emulsion Formulation on Particle Size and Stability[J]. Transportation Research Record, 2023, 2677(1): 587-598.
[26] Wang D, Hu L, Dong S, et al. Assessment of testing methods for higher temperature performance of emulsified asphalt[J]. Journal of Cleaner Production, 2022, 375: 134101.
[27] Jain S, Singh B. Cold mix asphalt: An overview[J]. Journal of Cleaner Production, 2021, 280: 124378.
[28] Al-Mohammedawi A, Mollenhauer K. Current research and challenges in bitumen emulsion manufacturing and its properties[J]. Materials, 2022, 15(6): 2026.
[29] Chen X, Wang H, Wang Q, et al. The Influence of Biomass Masut and Emulsifier on Emulsified Bio-asphalt Performance[C]//International Conference on Transportation Infrastructure and Materials 2017. 2017.
[30] Wang S, Chen X, Zhang X, et al. Effect of ionic emulsifiers on the properties of emulsified asphalts: An experimental and simulation study[J]. Construction and Building Materials, 2022, 347: 128503.
[31] Chen D, Zhou J, Zhang Q, et al. Evaluation methods and research progresses in bio-oil storage stability[J]. Renewable and Sustainable Energy Reviews, 2014, 40: 69-79.
[32] Jacobson K, Maheria K C, Dalai A K. Bio-oil valorization: A review[J]. Renewable and Sustainable Energy Reviews, 2013, 23: 91-106.
[33] Li H, Zhao H, Liao K, et al. A study on the preparation and storage stability of modified emulsified asphalt[J]. Petroleum science and technology, 2012, 30(7): 699-708.
[34] Ma Z, Wang H, Hui B, et al. Optimal design of fresh sand fog seal mortar using response surface methodology (RSM): Towards to its workability and rheological properties[J]. Construction and Building Materials, 2022, 340: 127638.
[35] Ma Z, Wang H, Li Y, et al. Performance-optimised design of sand fog seal for pavement cold repair using RSM I-optimal methodology[J]. International Journal of Pavement Engineering,

2023, 24(1): 2188592.
[36] Mohamed O A, Masood S H, Bhowmik J L. Characterization and dynamic mechanical analysis of PC-ABS material processed by fused deposition modelling: An investigation through I-optimal response surface methodology[J]. Measurement, 2017, 107: 128-141.
[37] Goos P, Jones B, Syafitri U. I-optimal design of mixture experiments[J]. Journal of the American Statistical Association, 2016, 111(514): 899-911.
[38] Anderson-Cook C M, Borror C M, Montgomery D C. Response surface design evaluation and comparison[J]. Journal of Statistical Planning and Inference, 2009, 139(2): 629-641.
[39] Goos P, Jones B. Optimal design of experiments: a case study approach[M]. John Wiley & Sons, 2011.
[40] Derringer G, Suich R. Simultaneous optimization of several response variables[J]. Journal of quality technology, 1980, 12(4): 214-219.
[41] Candioti L V, De Zan M M, Cámara M S, et al. Experimental design and multiple response optimization. Using the desirability function in analytical methods development[J]. Talanta, 2014, 124: 123-138.
[42] Ingrassia L P, Cardone F, Canestrari F, et al. Experimental investigation on the bond strength between sustainable road bio-binders and aggregate substrates[J]. Materials and Structures, 2019, 52: 1-14.
[43] Ingrassia L P, Lu X, Ferrotti G, et al. Chemical, morphological and rheological characterization of bitumen partially replaced with wood bio-oil: Towards more sustainable materials in road pavements[J]. Journal of Traffic and Transportation Engineering (English Edition), 2020, 7(2): 192-204.
[44] Sorunmu Y, Billen P, Spatari S. A review of thermochemical upgrading of pyrolysis bio-oil: Techno-economic analysis, life cycle assessment, and technology readiness[J]. Gcb Bioenergy, 2020, 12(1): 4-18.
[45] Laird D A, Brown R C, Amonette J E, et al. Review of the pyrolysis platform for coproducing bio‐oil and biochar[J]. Biofuels, bioproducts and biorefining, 2009, 3(5): 547-562.
[46] Programme, U. N. E., 2020. 2020 Global Status Report For Buildings and Construction: Towards a Zero-Emission, Efficient and Resilient Buildings and Construction Sector. United Nations Environment Programme Nairobi, Kenya.
[47] Han Y, Li H, Liu J, et al. Life cycle carbon emissions from road infrastructure in China: A region-level analysis[J]. Transportation Research Part D: Transport and Environment, 2023, 115: 103581.
[48] Zhao W, Yang Q. Design and performance evaluation of a new green pavement: 100% recycled asphalt pavement and 100% industrial solid waste[J]. Journal of Cleaner Production, 2023, 421: 138483.
[49] Ning P, Yang G, Hu L, et al. Recent advances in the valorization of plant biomass[J]. Biotechnology for Biofuels, 2021, 14(1): 102.
[50] Lee S, Shah Y T. Biofuels and bioenergy: processes and technologies[M]. CRC Press, 2012.